Hindawi Publishing Corporation
Journal of Nanomaterials
Volume 2011, Article ID 798257, 5 pages
doi:10.1155/2011/798257

Research Article

Pulsed Current Activated Consolidation of Nanostructured Fe_3Al and Its Mechanical Property

Tae-Wan Kim,[1] In-Yong Ko,[1] Jung-Mann Doh,[2] Jin-Kook Yoon,[2] and In-Jin Shon[1,3]

[1] *Division of Advanced Materials Engineering, Research Center for Advanced Materials Development, Engineering College, Chonbuk National University, 664-14 Deokjin-dong 1-ga, Deokjin-gu, Jeonju, Jeonbuk 561-756, Republic of Korea*
[2] *Advanced Functional Materials Research Center, Korea Institute of Science and Technology, PO Box 131, Cheongryang, Seoul 130-650, Republic of Korea*
[3] *Department of Hydrogen and Fuel Cells Engineering, Specialized Graduate School, Chonbuk National University, Chonbuk, 561-756, Republic of Korea*

Correspondence should be addressed to In-Jin Shon, ijshon@chonbuk.ac.kr

Received 18 April 2010; Revised 30 May 2010; Accepted 14 June 2010

Academic Editor: William W. Yu

A nanopowder of Fe_3Al was synthesized from 3Fe and Al by high-energy ball milling. A dense nanostructured Fe_3Al was consolidated by pulsed current activated sintering method within 2 minutes from mechanically synthesized powders of Fe_3Al and horizontally milled powders of 3Fe+Al. The grain size, sintering behavior, and hardness of Fe_3Al sintered from horizontally milled 3Fe+Al powders and high-energy ball milled Fe_3Al powder were compared.

1. Introduction

Iron aluminide (Fe_3Al) is of interest for structural applications at elevated temperature in hostile environments. This is because it generally possess excellent oxidation and corrosion resistance, relatively lower density and lower material cost than Ni-based alloy [1, 2]. However, its use has been limited by its brittleness at room temperature. This drawback can be improved by grain size reduction. Nanocrystalline materials have received much attention as advanced engineering materials with improved physical and mechanical properties [3, 4]. As nanomaterials possess high strength, high hardness, excellent ductility, and toughness, undoubtedly, more attention has been paid for the application of nanomaterials [5, 6].

Conventional methods of processing iron aluminides, including melting and casting have been investigated till now [7, 8]. However, none of these methods yield nanostructures. In recent years, some efficient methods were reported to fabricate the fine grain size materials, such as mechanical alloying, pulsed current activated sintering [9, 10]. The mechanical alloying process, which involves a repeated cold-working, fracture, and welding, makes microstructure refinement and alloy formation. The pulsed current-activated sintering is a rapid consolidation processing method where uniform, dense, and fine grain materials can be obtained by applying pressures and passing pulsed current the compact. And the process, due to spark plasma formed between the powder particles, enhances the distorted energy of the particles and increases the rate of the diffusion between the particles [11–14].

The purpose of this study is to produce nanopowder of Fe_3Al and densify nanocrystalline Fe_3Al compound within two minutes from mixtures of 3Fe+Al powders and mechanically synthesized Fe_3Al, respectively, using this pulsed current activated sintering method and to evaluate its mechanical properties and grain size.

2. Experimental Procedures

Powders of 99.5% Fe (<10 μm, Alfa, Inc) and 99% pure Al (−200 mesh, Samchun Chemical, Inc) were used as a starting materials. 3Fe and Al powders ratio were mixed by two-type methods. Firstly, the powders were milled in a high-energy ball mill, Pulverisette-5 planetary mill with 250 rpm

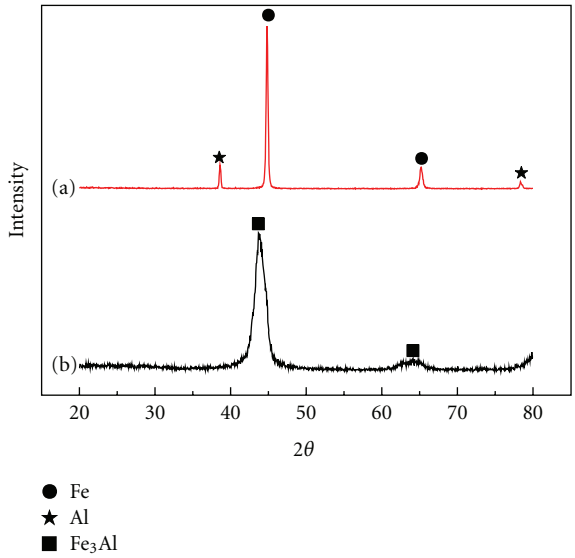

Figure 1: XRD patterns of milled powder: (a) horizontal milled 3Fe and Al powder, (b) high-energy ball milled Fe_3Al powder.

and for 10 hrs. Tungsten carbide balls (8.5 mm in diameter) were used in a sealed cylindrical stainless steel vial under argon atmosphere. The weight ratio of ball-to-powder was 30 : 1. Secondly, the powders were mixed in polyethylene bottles using zirconia balls with ethanol and the process was performed at a horizontal rotation velocity of 250 rpm for 10 h. The grain sizes of Fe_3Al were calculated using Suryanarayana and Grant Norton's formula [15]

$$B_r\left(B_{\text{crystalline}} + B_{\text{strain}}\right)\cos\theta = k\frac{\lambda}{L} + \eta\sin\theta, \quad (1)$$

where B_r is the full width at half-maximum (FWHM) of the diffraction peak after instrument correction; $B_{\text{crystalline}}$ and B_{strain} are FWHM caused by small grain size and internal stress, respectively; k is constant (with a value of 0.9); λ is wavelength of the X-ray radiation; L and η are grain size and internal strain, respectively; θ *is* the Bragg angle. The parameters B and B_r follow Cauchy's form with the relationship: $B = B_r + B_s$, where B and B_s are FWHM of the broadened Bragg peaks and the standard sample's Bragg peaks, respectively.

After milling, the mixed powders were placed in a graphite die (outside diameter, 45 mm; inside diameter, 20 mm; height, 40 mm) and then introduced into the pulsed current activated sintering system made by Eltek in South Korea [9]. The four major stages in the synthesis are as follows. The system was evacuated (stage 1). And a uniaxial pressure of 80 MPa was applied (stage 2). A pulsed current (on time: 20 μs; off time: 10 μs) was then activated and maintained until densification was attained as indicated by a linear gauge measuring the shrinkage of the sample (stage 3). Temperature was measured by a pyrometer focused on the surface of the graphite die. At the end of the process, the sample was cooled to room temperature (stage 4).

The relative densities of the synthesized sample were measured using the Archimedes method. Microstructural information was obtained from product samples which were polished and etched using a solution of H_2SO_4 (20 vol.%) and H_2O (80 vol.%) for 35 s at room temperature. Compositional and microstructural analyses of the products were made through X-ray diffraction (XRD) and scanning electron microscopy (SEM) with energy dispersive X-ray analysis (EDAX). Vickers hardness was measured by performing indentations at load of 20 kg and a dwell time of 15 s on the sintered samples.

3. Results and Discussion

XRD patterns of milled powder is shown in Figure 1. Fe_3Al was not synthesized during the horizontal rotation ball milling in ethanol, but synthesized during high-energy ball milling. The average grain size of Fe_3Al measured by Suryanarayana and Norton's formula [15] was 5 nm. Figure 2 shows FE-SEM image of Fe_3Al powder synthesized by high-energy ball milling and X-ray mapping of Fe and Al. From the X-ray mapping, Fe and Al were uniformly distributed and the particles of milled Fe_3Al shown in Figure 2 are bigger. I think the reason in milling processing, iron and aluminum powders were wrapped with each other by server plastic deformation, resulting in grain refinement and mechanical alloying.

The changes in shrinkage displacement and temperature of the surface of the graphite die with heating time during the processing of Fe-Al system are shown in Figure 3. As the pulsed current was applied, the shrinkage displacement of Fe_3Al continuously increased with temperature up to about 1000°C, but the shrinkage of 3Fe+Al gradually increased with temperature up to (A) point and then abruptly increased. When the reactant mixture of 3Fe and Al was heated under 80 MPa pressure to (A) point, no reaction took place as judged by subsequent XRD analysis. X-ray diffraction result, shown in Figure 4(a), exhibits only peaks pertaining to the Fe and Al. However, when the temperature was raised to 1150°C, the starting powders (3Fe+Al) reacted producing highly dense products (Fe_3Al), shown in Figure 4(b). The abrupt increase in the shrinkage displacement at the ignition temperature is due to the increase in density as a result of molar volume change associated with the formation of Fe_3Al from 3Fe and Al reactant and the consolidation of the product.

Figure 5 shows FE-SEM images of Fe_3Al sintered from (a) horizontally milled Fe+Al powders and (b) high-energy ball milled Fe_3Al powder. The grain size of Fe_3Al sintered from high-energy ball milled Fe_3Al is smaller than that of Fe_3Al sintered from horizontally milled 3Fe+Al powders. The grain size of Fe_3Al sintered from high-energy ball milled Fe_3Al and from horizontally milled 3Fe+Al powders are about 40 nm and 300 nm, respectively. And the corresponding relative density of Fe_3Al are 97% and 96%, respectively. The grain size of Fe_3Al sintered from horizontally milled 3Fe+Al powders is higher than that of Fe_3Al sintered from high-energy ball milled Fe_3Al because Fe_3Al can have grain growth due to exothermic energy when Fe_3Al synthesized from 3Fe and Al during the sintering.

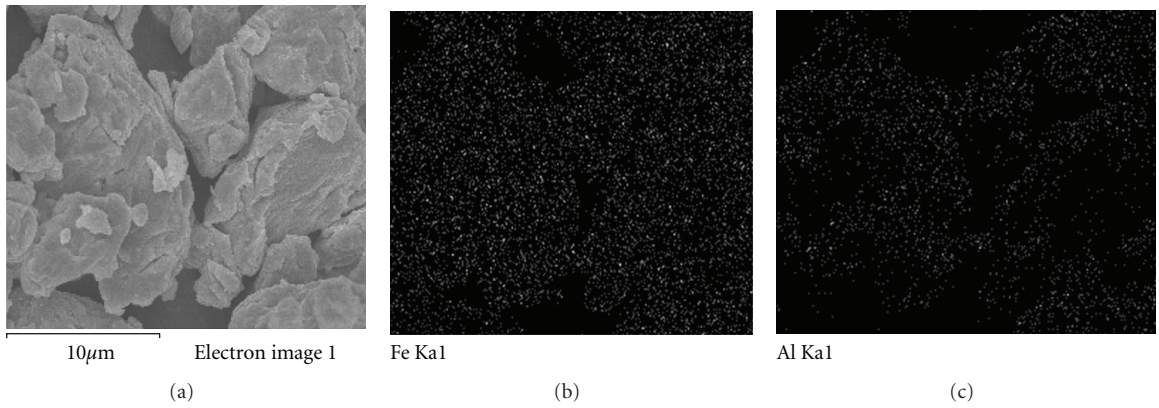

FIGURE 2: FE-SEM image of Fe_3Al and X-ray mapping of Fe and Al in high-energy ball milled powder.

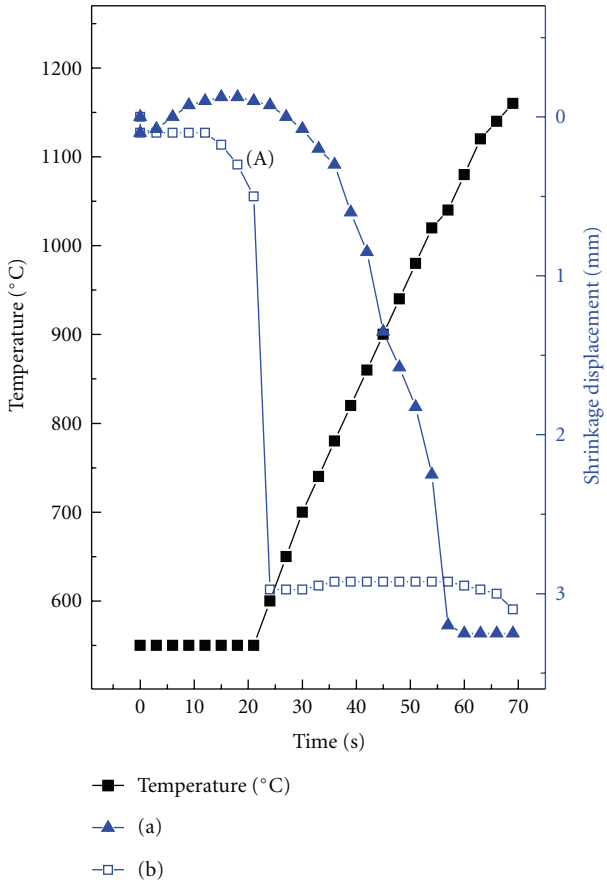

FIGURE 3: Variations of temperature and shrinkage displacement with heating time during pulsed current activated sintering of Fe-Al system: (a) high-energy ball milled Fe_3Al powder, (b) horizontal milled 3Fe and Al powder.

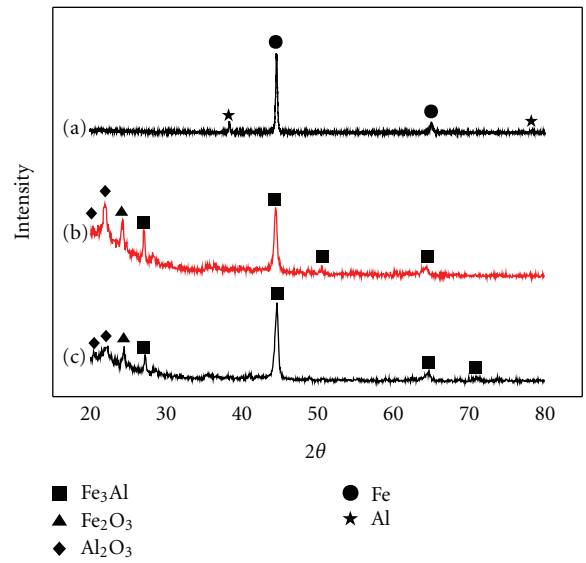

FIGURE 4: XRD patterns of the Fe-Al system: (a) sample heated to (A) point (b) heated to 1150°C from horizontal milled 3Fe and Al powder, (c) heated to 1150°C high-energy ball milled Fe_3Al powder.

The average grain size of the sintered Fe_3Al is not greatly larger than that of the initial powder, indicating the absence of great grain growth during sintering. This retention of the grain size is attributed to the high-heating rate and the relatively short-term exposure of the powders to the high temperature. The role of the current (resistive or inductive) in sintering and or synthesis has been focus of several attempts aimed at providing an explanation to the observed enhancement of sintering and the improved characteristics of the products. The role played by the current has been variously interpreted, the effect being explained in terms of fast heating rate due to Joule heating, the presence of plasma in pores separating powder particles [16], and the intrinsic contribution of the current to mass transport [17–19].

Vickers hardness measurements were made on polished sections of the Fe_3Al using a 20 kg_f load and 15 s dwell time. The calculated hardness values of Fe_3Al sintered from (a) horizontally milled 3Fe+Al powders and (b) high energy ball milled Fe_3Al powder were 317 kg/mm^2 and 458 kg/mm^2, respectively. This value represents an average of five measurements. Cracks were not observed to propagate from the indentation corner. So, fracture toughness cannot be calculated from crack length. The hardness of Fe_3Al sintered

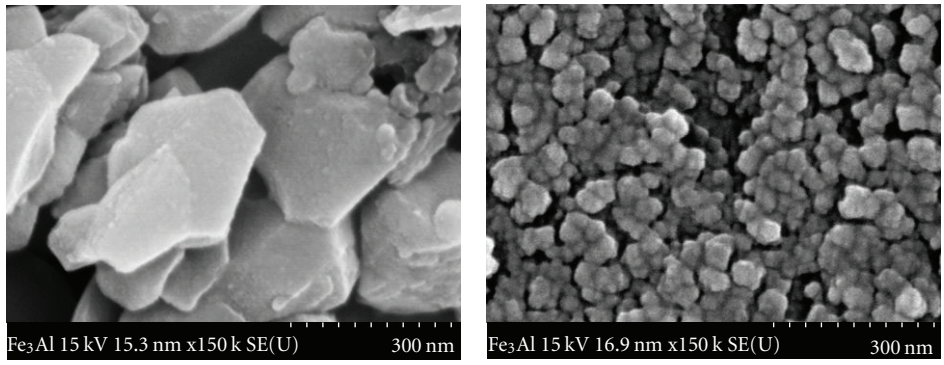

(a) (b)

Figure 5: FE-SEM images of Fe_3Al sintered at 1150°C: (a) horizontal milled 3Fe and Al powder, (b) high-energy ball milled Fe_3Al powder.

from high-energy ball milled Fe_3Al is higher than that of Fe_3Al sintered from horizontally milled 3Fe+Al powders due to refinement of grain and high density. Zhang and Liu investigated Fe_3Al prepared by vacuum induction melting followed by hot spinning forging. The hardness of Fe_3Al was about 270 Kg/mm^2 [20]. The hardness of this study is higher than that of Zhang's work due to refinement of grain size.

4. Conclusions

Using the pulsed current activated sintering method, the densification of nanostructured Fe_3Al was accomplished from mechanically synthesized powder of Fe_3Al and milled 3Fe+Al powders. Nearly full density of Fe_3Al can be achieved within duration of 2 minutes for the applied pressure of 80 MPa and the pulsed current. The average grain sizes of Fe_3Al prepared by pulsed current activated sintering method from horizontally milled 3Fe+Al powders and high-energy ball milled Fe_3Al powder were about 300 nm and 40 nm, respectively. The calculated hardness values of Fe_3Al sintered from horizontally milled 3Fe+Al powders and high-energy ball milled Fe_3Al powder were 317 kg/mm^2 and 458 kg/mm^2, respectively.

Acknowledgments

This work was supported by New & Renewable Energy R&D program (2009T00100316) under the Ministry of Knowledge Economy, Republic of Korea.

References

[1] C. T. Liu, E. P. George, P. J. Maziasz, and J. H. Schneibel, "Recent advances in B2 iron aluminide alloys: deformation, fracture and alloy design," *Materials Science and Engineering A*, vol. 258, no. 1-2, pp. 84–98, 1998.

[2] S. C. Deevi and V. K. Sikka, "Nickel and iron aluminides: an overview on properties, processing, and applications," *Intermetallics*, vol. 4, no. 5, pp. 357–375, 1996.

[3] M. S. El-Eskandarany, "Structure and properties of nanocrystalline TiC full-density bulk alloy consolidated from mechanically reacted powders," *Journal of Alloys and Compounds*, vol. 305, no. 1-2, pp. 225–238, 2000.

[4] L. Fu, L. H. Cao, and Y. S. Fan, "Two-step synthesis of nanostructured tungsten carbide-cobalt powders," *Scripta Materialia*, vol. 44, no. 7, pp. 1061–1068, 2001.

[5] K. Kondoh, T. Threrujirapapong, H. Imai, J. Umeda, and B. Fugetsu, "CNTs/TiC reinforced titanium matrix nanocomposites via powder metallurgy and its microstructural and mechanical properties," *Journal of Nanomaterials*, vol. 2008, no. 1, Article ID 127538, 4 pages, 2008.

[6] S. Berger, R. Porat, and R. Rosen, "Nanocrystalline materials: a study of WC-based hard metals," *Progress in Materials Science*, vol. 42, no. 1–4, pp. 311–320, 1997.

[7] V. K. Sikka, in *Proceedings of the 5th Annual Conference on Fossil Energy Materials*, p. 197, Oak Ridge, Tenn, USA, 1991.

[8] J. R. Knibloe, R. N. Wright, and V. K. Sikka, in *Advanceds in Powder Metallurgy*, E. R. Andreotti and P. J. McGreehan, Eds., p. 219, Metal Powder Industries Federation, Princeton, NJ, USA, 1990.

[9] S.-K. Bae, I.-J. Shon, J.-M. Doh, J.-K. Yoon, and I.-Y. Ko, "Properties and consolidation of nanocrystalline $NbSi_2$-SiC-Si_3N_4 composite by pulsed current activated combustion," *Scripta Materialia*, vol. 58, no. 6, pp. 425–428, 2008.

[10] I.-J. Shon, D.-K. Kim, K.-T. Lee, and K.-S. Nam, "Properties and consolidation of nanostructured $Ce_{0.8}Gd_{0.2}O_{1.9}$ by pulsed-current-activated sintering," *Metals and Materials International*, vol. 14, no. 5, pp. 593–598, 2008.

[11] Z. Shen, M. Johnsson, Z. Zhao, and M. Nygren, "Spark plasma sintering of alumina," *Journal of the American Ceramic Society*, vol. 85, no. 8, pp. 1921–1927, 2002.

[12] J. E. Garay, S. C. Glade, U. Anselmi-Tamburini, P. Asoka-Kumar, and Z. A. Munir, "Electric current enhanced defect mobility in Ni_3Ti intermetallics," *Applied Physics Letters*, vol. 85, no. 4, pp. 573–575, 2004.

[13] J. R. Friedman, J. E. Garay, U. Anselmi-Tamburini, and Z. A. Munir, "Modified interfacial reactions in Ag-Zn multilayers under the influence of high DC currents," *Intermetallics*, vol. 12, no. 6, pp. 589–597, 2004.

[14] J. E. Garay, U. Anselmi-Tamburini, and Z. A. Munir, "Enhanced growth of intermetallic phases in the Ni-Ti system by current effects," *Acta Materialia*, vol. 51, no. 15, pp. 4487–4495, 2003.

[15] C. Suryanarayana and M. Grant Norton, *X-Ray Diffraction: A Practical Approach*, Plenum Press, New York, NY, USA, 1998.

[16] Z. Shen, M. Johnsson, Z. Zhao, and M. Nygren, "Spark plasma sintering of alumina," *Journal of the American Ceramic Society*, vol. 85, no. 8, pp. 1921–1927, 2002.

[17] J. E. Garay, S. C. Glade, U. Anselmi-Tamburini, P. Asoka-Kumar, and Z. A. Munir, "Electric current enhanced defect mobility in Ni_3Ti intermetallics," *Applied Physics Letters*, vol. 85, no. 4, pp. 573–575, 2004.

[18] J. R. Friedman, J. E. Garay, U. Anselmi-Tamburini, and Z. A. Munir, "Modified interfacial reactions in Ag-Zn multilayers under the influence of high DC currents," *Intermetallics*, vol. 12, no. 6, pp. 589–597, 2004.

[19] J. E. Garay, U. Anselmi-Tamburini, and Z. A. Munir, "Enhanced growth of intermetallic phases in the Ni-Ti system by current effects," *Acta Materialia*, vol. 51, no. 15, pp. 4487–4495, 2003.

[20] Z.-R. Zhang and W.-X. Liu, "Mechanical properties of Fe_3Al-based alloys with addition of carbon, niobium and titanium," *Materials Science and Engineering A*, vol. 423, no. 1-2, pp. 343–349, 2006.